Generic and simplified HV DC circuit breaker models for grid-level studies

Mario Zaja, Dragan Jovcic
School of Engineering
University of Aberdeen
Aberdeen, UK

Linash Kunjumuhammed,
Mitsubishi Electric Europe,
UK

Kazuyori Tahata, Takashi Inagaki
Mitsubishi Electric Corporation,
Japan

Simon Nee,
SciBreak AB,
Sweden

***Abstract* — This paper presents simplified and generic models for three DCCB topologies: hybrid DCCB, active current injection DCCB and VARC (VSC assisted) DCCB. The generic model has identical structure for all topologies, but topology-specific parameters. This generic modeling approach simplifies DC grid studies and enables fast comparison between different DCCB topologies and protection system configurations. Simulation results on a DC grid model in PSCAD indicate that generic DCCB model gives accurate basic variables (peak current and voltage) for all topologies. The simplified models show very good accuracy for most variables but may not be able to represent internal component stresses. The comparison between simulation times indicates significant benefit in using generic and simplified DCCB models over the more detailed counterparts.**

***Index Terms*— DC grid protection, DC circuit breaker, hybrid, mechanical, VSC assisted**

I. Introduction

Recent advancements in multi-terminal DC transmission have to a large extent been driven by the development of modern DC circuit breakers (DCCBs) [1]. Several DCCB topologies have been introduced in the recent years, including the hybrid [2], active current injection [3] and VSC-assisted [4, 5] DCCB. The operation of these devices has been successfully demonstrated on high voltage (HV) prototypes in laboratory conditions [2, 3, 5] while some have been installed in the field [1].

The ability to evaluate transient performance of DC grids using electromagnetic transient (EMT) simulation tools is of utmost importance to grid planners, transmission system operators and researchers. Detailed models of hybrid and mechanical DCCBs for EMT simulation software are developed in [6, 7] and provide a trustworthy representation of these circuit breaker topologies. However, the complexity of these models is fairly high which limits their applicability in grid-level studies. Even relatively simple grid models, say 4-10 terminals, can contain a large number of DCCB units, particularly in symmetrical monopole and bipole systems where both poles are energized. Utilizing detailed DCCB models in such an environment leads to excessive computing resource usage and very slow simulation speed.

Another challenge in DCCB modelling comes from significant differences between DCCB topologies [8, 9]. These differences, manifested in both the electrical and control system layout of the breaker, make it difficult to perform side-by-side comparison of grid protection strategies utilizing different DCCB types. This problem is especially prominent in preliminary studies where the DCCB topology has not been selected yet. For grid planning operations in particular, a black-box DCCB model would be highly beneficial in providing a quick and simple way to determine basic component specifications and requirements.

This paper proposes generic, simplified models suitable for widely different DC CB topologies, and for fast large-scale grid-level studies in EMT simulation software. The features and limitations of the proposed models are discussed while their accuracy and complexity is assessed by comparing the models' responses in PSCAD.

II. Models of common DCCB topologies

A. Simplified and Generic model of Hybrid DCCB

The operation of a hybrid DCCB (HCB) and the functionality of each component is well understood and explained in [6, 9, 10]. The HCB utilizes a low-loss auxiliary branch to carry the current in closed state and a HV semiconductor valve for current interruption. The breaker topology is shown in Fig. 1. Key HCB components are the di/dt limiting inductor L_{dc}, residual current breaker (RCB), ultrafast disconnector (UFD), load commutation switch (LCS), main breaker (MB) and the energy absorber (EA).

The MB, EA and, to a lesser extent LCS, physically consists of a large number of unit components (IGBTs and surge arresters). Because of non-linear component modelling, the detailed HCB model provides a very accurate response under all operating conditions. However, solving electrical circuits with non-linear components is very computationally intensive because the admittance matrix needs to be recalculated in every time step.

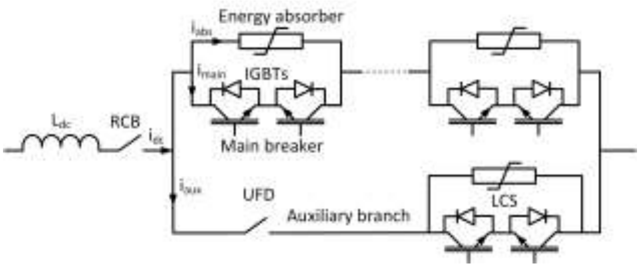

Fig. 1. Detailed equivalent HCB model

The detailed equivalent model (shortly "detailed") utilizes the same topology from Fig. 1. However, the MB, EA and LCS are represented as single-component equivalents with lumped parameters. Nevertheless, the modularity of the main branch is preserved and the branch consists of several breaker units. This is important as it enables the simulation of fault current limiting (FCL) mode [6]. Both the IGBTs and arresters are modelled using non-linear or piecewise-linear components readily available in the simulation software.

The remainder of the components from Fig. 1 (L_{dc}, RCB, UFD and LCS' arrester) are physically implemented as a single unit which is reflected in the model. The UFD and RCB are modelled as non-ideal switches with an opening/closing time delay and specific current breaking capability.

The simplified HCB model shown in Fig. 2 replaces all the semiconductors of the detailed model with non-ideal switches. Within EMT software, a non-ideal switch is implemented as a two-state variable resistor with very low resistance in the closed state and very high resistance in the open state. This makes the switch a lot easier to solve since the admittance matrix is recalculated only when the state of the switch changes.

Despite the simplification of semiconductor components, the simplified HCB model is still capable of accurately estimating the conduction losses and temperature of semiconductor switches. This is possible because the series resistance of the breaker has negligible influence on the breaker current in closed state. Branch currents, used as the inputs for the power loss estimation, are virtually unaffected by the differences in switch representation. Since the modularity of the breaker is preserved, the simplified HCB model can also simulate FCL operation.

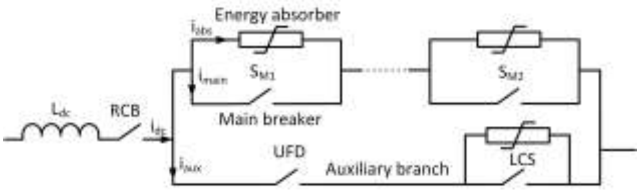

Fig. 2. Simplified HCB model

The generic DCCB model, shown in Fig. 3, is the simplest of all models and can represents any DCCB topology. The common components of all DCCB topologies (L_{dc}, RCB and EA) are modelled individually using lumped parameters while the branches for current conduction and interruption are reduced to a single non-ideal switch S_{BRK}. The operating time of S_{BRK} is equal to the fault neutralization time of the DCCB. In the context of a HCB, S_{BRK} unifies the auxiliary and the main branch. Because the turn-off time of MB is negligible, the opening time of S_{BRK} is equal to the opening time of the UFD.

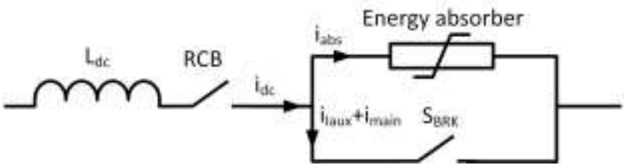

Fig. 3. Generic DCCB model

The generic DCCB model is very simple to solve since only a single non-linear component is used (EA) while the number of switches is reduced to two. On the downside, modularity of the breaker is not preserved which leads to reduced functionality.

A comparison between the functionalities of the three HCB models is shown in Table I. The simplified model has most of the features of the detailed model with slightly reduced accuracy in some cases. The generic model on the other hand has significantly reduced functionality.

TABLE I. FUNCTIONALITIES OF DIFFERENT HCB MODELS

	Detailed	Simplified	Generic
Current breaking	Yes	Yes	Yes
Fault current limiting	Yes	Yes	No
Individual branch currents	All	All	Some
Power loss estimation	Yes	Yes	No
Switch temperature estimation	Yes	Yes	No
Arrester energy estimation	Yes	Yes	Yes
LCS stress	Yes	Yes	No
Self-protection	Full	Full	Limited
Failure modes	All	Most	Few

B. Active current injection DCCB

Active current injection DCCB creates artificial zero crossing by superimposing resonant current from current injection branch on DC current and interrupts DC current [4, 10]. This DCCB consists of mechanical interrupters in parallel with series connection of an inductor (L_p), a pre-charged capacitor (C_p) and high-speed making switches (HSMS). The breaker topology for HVDC application is shown in Fig. 4. For HVDC application, main interrupters (MI) and HSMSs are connected in series in order to increase withstand voltage of the breaker. In addition, voltage grading impedances are required to ensure distribution of voltage stress across MIs.

In the detailed active current injection DCCB model, each MI unit and HSMS unit is modeled individually. This makes it possible to perform the simulation with MI unit operation delay or failure. It is also possible to check voltage stress on each MI unit.

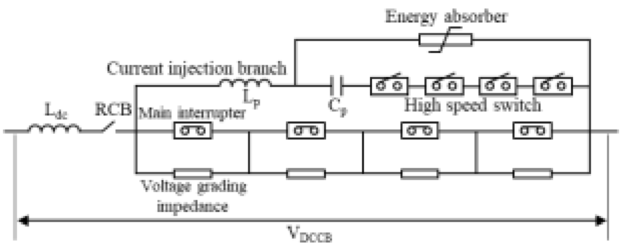

Fig. 4. Detailed active current injection DCCB model

Active current injection DCCB model can be simplified as shown in Fig. 5. MIs are represented by single ideal switch. L_p, HSMS and voltage grading impedance are removed from this model. As the simplified model keeps C_p, this model can represent the interaction between HVDC system and C_p after the fault interruption. As the number of elements in the simplified active current injection DCCB model is small, this model can shorten the total simulation time. Therefore, this model is adequate for HVDC system simulation when the detailed DCCB operation mode or voltage stress information of each unit is not necessary.

The generic DCCB model shown in Fig. 3 is applicable for active current injection DCCB also. Since C_p is removed, this model may not accurately represent current and voltage behavior just after the fault. Therefore, this model is adequate to estimate fault current peak, DCCB voltage peak or total arrester energy. Table II summarize a comparison between the functionalities of the active current injection DCCB models.

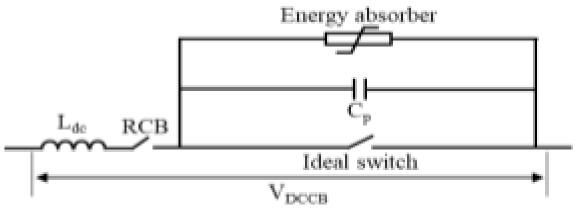

Fig. 5. Simplified active current injection DCCB model

TABLE II. FUNCTIONALITIES OF DIFFERENT ACTIVE CURRENT INJECTION DCCB MODELS

	Detailed	Simplified	Generic
Current breaking	Yes	Yes	Yes
Arrester energy estimation	Yes	Yes	Yes
Failure modes	All	Few	Few
Voltage stress on each unit	Yes	No	No
C_p influence on system	Yes	Yes	No

C. VSC-Assisted Resonant Current DCCB

To interrupt current, the VSC-Assisted Resonant Current (VARC) DCCB relies on a low-voltage VSC to successively increase the amplitude of the current in a resonant circuit that is connected in parallel with the main interrupter [4, 5]. When the amplitude of the resonant circuit current is equal to that of the line current, a current zero-crossing occurs in the main interrupter, which then leads to commutation of the line current into the surge arrester and subsequently suppression of the fault current. The circuit diagram for a VARC DCCB module is shown in Fig. 6 below.

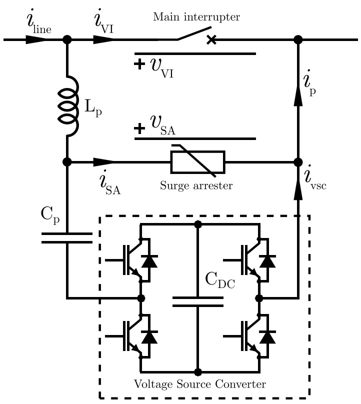

Fig. 6. Main circuit diagram of a VARC DCCB module

These breaker modules can be connected in series, as shown in Fig. 7, to reach sufficient TIV of the circuit breaker. For modelling of this circuit breaker, a fully detailed model containing the components in Fig. 6 and Fig. 7 can be used. Such a model is primarily useful for understanding the behavior of the breaker main circuit, and the stresses on its subcomponents.

The detailed model of the circuit breaker requires simulation at a very short timestep of approximately 1 µs in order to correctly model the performance. Such a short timestep is far from necessary to simulate system level dynamics. From a system perspective, there is also little reason to model the breaker with all details, since the circuit breaker has a nearly zero impedance until a current zero-crossing has been reached in the main interrupter of the breaker. At that point, only the surge arrester and the resonant circuit capacitor contribute to the voltage seen across the circuit breaker.

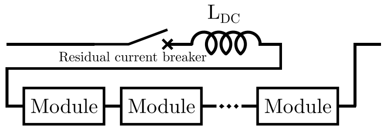

Fig. 7. VARC DCCB circuit diagram. The module block contains the circuit shown in Fig. 6.

After the suppression of the fault current has been completed, a resonance on the order of 300 A and 500 Hz between the resonant circuit capacitor and the current limiting reactor ensues. This oscillation is also visible from the outside system. The resonant circuit inductor and the entire VSC can, however, be excluded from the model for all system level studies. Under the assumption that the modules of the breaker are identical, the stack of modules can be replaced by one large equivalent unit without changing the system-level behavior of the breaker. Such a model is then the same as the one proposed for the active current injection DCCB and shown in Fig. 5, but likely with different component values.

A generic DCCB model also neglects the effect of the capacitor in the resonant circuit, as shown in Fig. 3. This primarily has the two visible effects that the rate of rise of the voltage across the surge arrester during interruption becomes instantaneous, and that the small current oscillation after interruption is neglected. A summary of the capabilities of the three different models is compiled in Table III.

Table III. FUNCTIONALITIES OF DIFFERENT VARC DCCB MODELS

	Detailed	Simplified	Generic
Current breaking	Yes	Yes	Yes
Power loss estimation	Yes	Yes	Yes
Arrester energy estimation	Yes	Yes	Yes
Failure modes	All	Few	Few
Voltage stress on each unit	Yes	No	No
C_p influence on system	Yes	Yes	No

III. TEST SYSTEM

Evaluation of DCCB models is performed on a four-terminal DC grid model used in the PROMOTioN project. The test system is shown in Fig. 8 and described in detail in [11]. Each MMC is rated for 1265 MVA while the voltage level is ±320 kV in a symmetrical monopole configuration. Sixteen breaker units are used in total, two at the end of each cable. Fault detection is performed using a fast hybrid method based on voltage and current measurements. The method, also described in [11], provides very fast fault detection with the response time below 1 ms.

In the following tests, a solid pole-to-pole fault is applied at the MMC 1 side of cable 12 (as indicated in Fig. 8) at 0.8 s. This is the most severe condition in terms of fault current. DCCB opening is initiated as soon as the fault is detected while the current and voltage responses of DCCBs 12 and 21 are monitored. Positive current direction is towards the center of the cable. A comparison of DCCB current and voltage across the breaker is made between different models of the same DCCB topology, characterized by identical DCCB inductor size and opening time. Table IV summarizes the parameters of each DCCB topology used in the simulation. Note that value of the C_p in the model is provided for the simulation purposes. The value for the product will be determined depending on the system configuration and customer specification

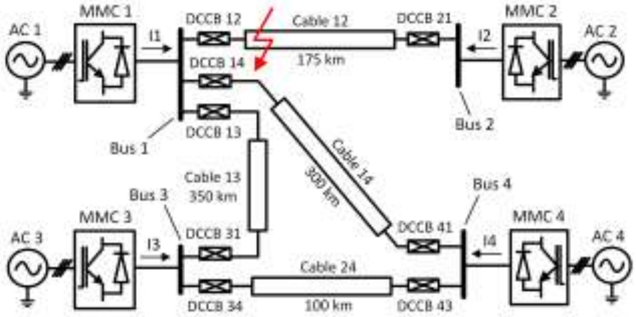

Fig. 8. Four terminal DC grid test system

TABLE IV. SIMPLIFIED AND GENERIC DCCB MODEL PARAMETERS

Parameter	Hybrid	Active current injection	VARC
T_{BRK}	2 ms	8 ms	2 ms
T_{RCB}	30 ms	30 ms	30 ms
C_p (simplified only)	0	5 µF	600 nF
L_{dc}	100 mH	100 mH	100 mH

IV. SIMULATION RESULTS

A. Hybrid DCCB

The main branch of the HCB consists of four 80 kV units. Current and voltage responses of DCCBs 12 and 21 are compared in Fig. 9 between the three investigated HCB models. The measured breaker voltage includes the voltage across L_{dc}. As visible from the figure, the system-level responses of all three models are virtually identical. It is concluded that the HCB model selection can be based solely on the functional requirements outlined in Table I.

B. Active current injection DCCB

The main branch of detailed active current injection DCCB model consists of four 80 kV units. Current and voltage response of DCCBs 12 and 21 are compared in Fig. 10 between the three investigated DCCB models. As shown in Fig. 10, the system-level responses of the detailed model and simplified model are almost the same. On the other hand, the generic model slightly lower DCCB voltage after the fault current suppression. In conclusion, the simplified model and the detailed model can be applied for system-level simulation with the active current injection DCCB. The generic model is also applicable when the purpose of the system-level simulation is to estimate only the peak value of fault current, DCCB voltage and arrester energy.

C. VSC-Assisted Resonant Current DCCB

The main branch of the detailed VARC model consists of four 80 kV units. A comparison between the current and voltage responses of different DCCB models is shown in Fig. 11. While all three models yield similar peak DC current, the generic DCCB model does not represent the oscillating current behavior following the current suppression period. The detailed model provides a different transient voltage waveform in Fig. 11 (b) during the fault current suppression period. However, it was necessary to solve this model using a smaller time step (1 µs) which may have had an influence. The generic model produces a jump in DCCB voltage following RCB opening which is not observed with the other two models. It is concluded that only the detailed model can accurately represent the voltage transients while the current transient is sufficiently accurate with the simplified model.

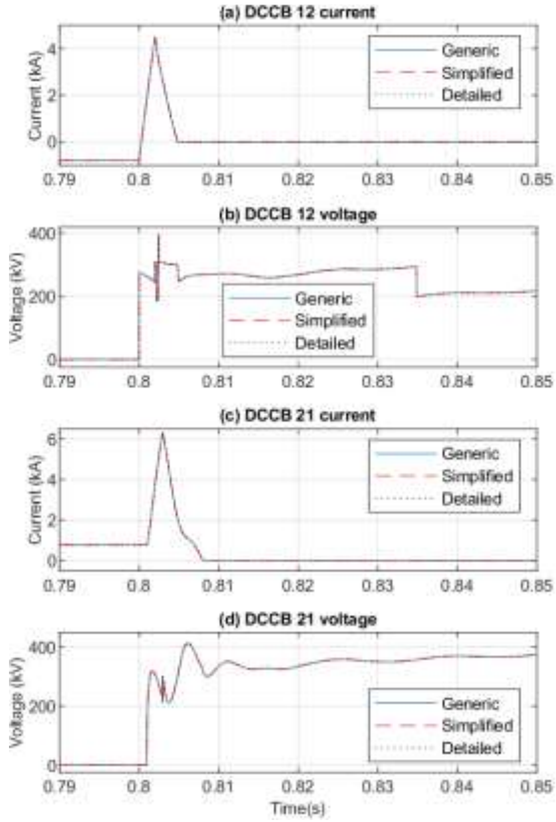

Fig. 9. Voltage and current responses of three HCB models

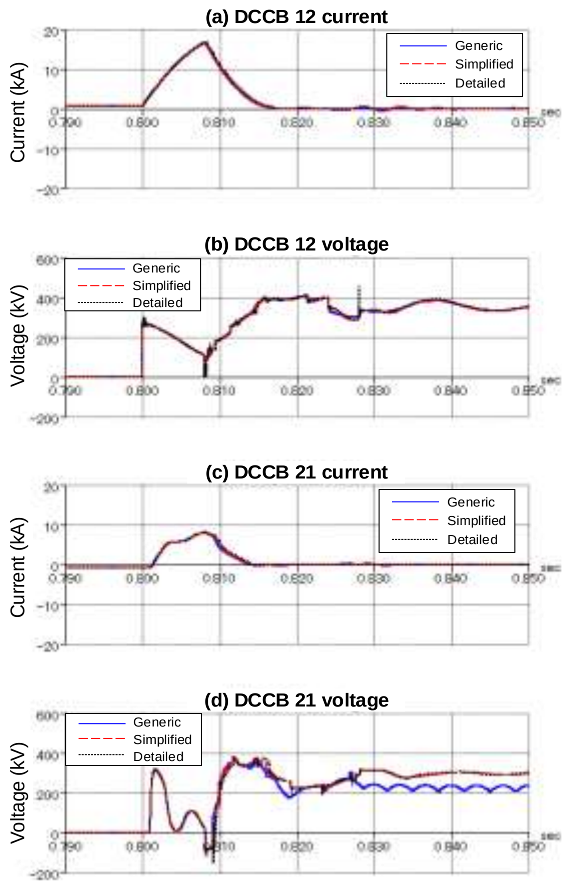

Fig. 10 Voltage and current responses of three active current injection DCCB models

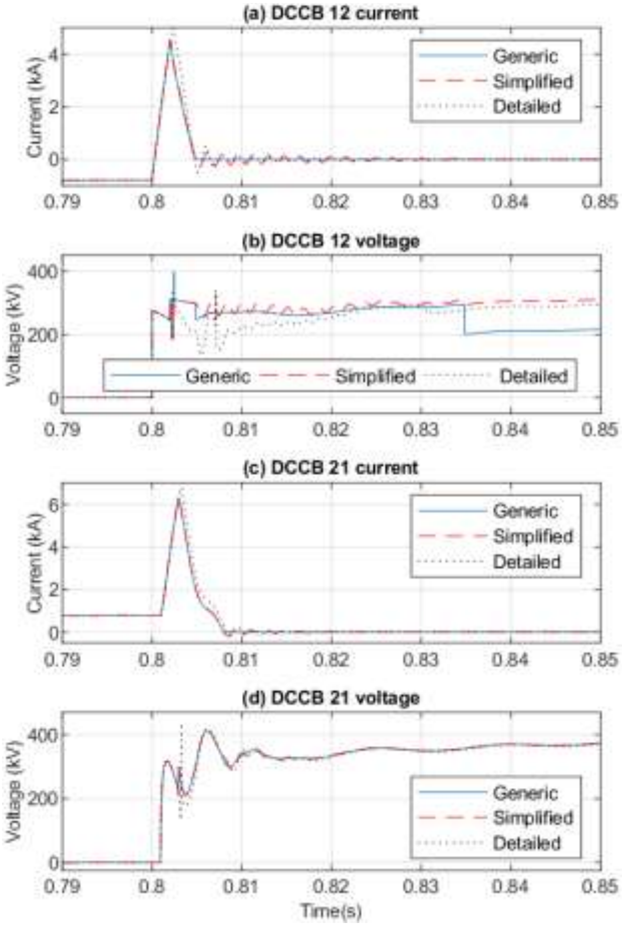

Fig. 11 Voltage and current responses of three VARC DCCB models

D. Simulation time comparison

The practicality of utilizing the examined DCCB models for grid-level studies is assessed by measuring the time it takes to simulate a 1 second simulation case on a typical office PC (3.1 GHz 4-core CPU, 8 GB RAM). The baseline test scenario is described in section III. The grid model is implemented in PSCAD with the simulation time step set to 10 µs. Corresponding DCCB model is used for all the 16 DCCB units in the grid. All the other aspects of the simulation model are identical in all cases.

A comparison between simulation times of the test scenario with different DCCB models is given in Table V. It is evident that DCCB model selection has a tremendous impact on the computational complexity of the test case, particularly in the case of HCB topology where the detailed model produces unreasonably long simulation times. The simplified HCB model greatly improves simulation speed, but the test case still takes 10x longer to solve compared to the generic model. This is attributed to the higher number of non-linear surge arresters used in the model (4 versus 1).

In case of a detailed VARC model, the simulation time step had to be decreased from 10 to 1 µs in order to obtain an accurate response and this factor also contributed to the prolonging of simulation time. In case of an active current injection DCCB model, the number of elements is smaller than that of the HCB or VARC model and there is only several minutes difference between simulation times. The simplified and generic models for the active current injection and VARC topology yield identical simulation times so the simplified model is preferred due to increased accuracy.

TABLE V. SIMULATION TIMES OF DIFFERENT DCCB MODELS

Topology	Detailed	Simplified	Generic
HCB	690 min ~ 11.5 h	25 min	2.5 min
Active current injection	6.0 min	2.5 min	2.5 min
VARC	197 min ~ 3.3 h	2.5 min	2.5 min

V. CONCLUSION

The paper concludes that detailed modeling may not be necessary for any of the considered DCCB topologies: hybrid DCCB, active current injection DCCB and VARC DCCB, when applied in system level studies. The proposed generic gives accurate basic variables (peak current and voltage) for all DCCB topologes which should be adequate for basic studies. The model is also very easy to implement and only requires the knowledge of the opening/closing time of the switches. The simplified model shows improved accuaracy for most variables but may not be able to represent internal component stresses. The comparison of similation times indicates significnat benefit in using generic or simplified DCCB models over detailed ones.

ACKNOWLEDGEMENTS

This work was supported by the European Union's Horizon 2020 research and innovation program under grant No. 691714.

REFERENCES

[1] D. Jovcic, G. Tang, and H. Pang, "Adopting Circuit Breakers for High-Voltage dc Networks: Appropriating the Vast Advantages of dc Transmission Grids," *IEEE Power Energy Mag.*, vol. 17, no. 3, pp. 82–93, May 2019.

[2] J. Hafner and B. Jacobson, "Proactive Hybrid HVDC Breakers - A key innovation for reliable HVDC grids," in *The electric power system of the future - Integrating supergrids and microgrids, International Symposium*, 2011, pp. 1–9.

[3] K. Tahata *et al.*, "HVDC circuit breakers for HVDC grid applications," in *AC and DC Power Transmission, 11th IET International Conference on*, 2015, pp. 1–9.

[4] L. Angquist, S. Norrga, T. Modeer, and S. Nee, "Fast HVDC breaker using reduced-rating power electronics," in *13th IET International Conference on AC and DC Power Transmission (ACDC 2017)*, 2017, pp. 31 (6 .)-31 (6 .).

[5] L. Ängquist, S. Nee, T. Modeer, A. Baudoin, S. Norrga, and N. A. Belda, "Design and test of VSC assisted resonant current (VARC) DC circuit breaker," in *15th IET International Conference on AC and DC Power Transmission (ACDC 2019)*, 2019, pp. 34 (6 pp.)-34 (6 pp.).

[6] D. Jovcic, S. Nguefeu, W. Lin, and H. Saad, "Modelling of high-power hybrid DC circuit breaker for grid-level studies," *IET Power Electron.*, vol. 9, no. 2, pp. 237–246, Feb. 2016.

[7] W. Lin, D. Jovcic, S. Nguefeu, and H. Saad, "Modelling of high power mechanical DC circuit breaker," in *Power and Energy Engineering Conference (APPEEC), 2015 IEEE PES Asia-Pacific*, 2015, pp. 1–5.

[8] D. Jovcic, A. Jamshidifar, M. Popov, and S. Liu, "Modelling and Comparison of Common Functionalities of HVDC Circuit Breakers," in *2018 IEEE Power & Energy Society General Meeting (PESGM)*, 2018, pp. 1–5.

[9] C. M. Franck et al., "Technical requirements and specifications of state-of-the-art HVDC switching equipment." CIGRE WG A3/B4.34, Report No. 683, 2017.

[10] R. Derakhshanfar, T. U. Jonsson, U. Steiger, and M. Habert, "Hybrid HVDC breaker – A solution for future HVDC system," in *CIGRE Session 2014*, 2014, pp. 1–12.

[11] W. Leterme et al., "Broad comparison of fault clearing strategies for DC grids," PROMOTioN Deliverable 4.2, www.promotion-offshore.net, 2017.